RETRIEVAL OF ATMOSPHERIC AND SURFACE PARAMETERS FROM AIRS/AMSU/HSB DATA UNDER CLOUDY CONDITIONS

Joel Susskind[1], Chris Barnet[2], and John Blaisdell[3]

1. NASA/GSFC, Code 910.4, Greenbelt, MD 20771
2. Joint Center for Earth Systems Technology, NASA/GSFC, Code 910.4, Greenbelt, MD 20771
3. Science Applications International Corporation, NASA/GSFC, Code 910.4, Greenbelt, MD 20771

Popular Summary

New state of the art methodology is described to analyze AIRS/AMSU/HSB data in the presence of multiple cloud formations. The methodology forms the basis for the AIRS Science Team algorithm which will be used to analyze AIRS/AMSU/HSB data on EOS Aqua. Results are shown for AIRS Science Team simulation studies with multiple cloud formations. These simulation studies imply that clear column radiances can be reconstructed under partial cloud cover with an accuracy comparable to single spot channel noise in the temperature and water vapor sounding regions, temperature soundings can be produced under partial cloud cover with RMS errors on the order of, or better than, 1°K in 1 km thick layers from the surface to 700 mb, 1 km layers from 700 mb to 300 mb, 3 km layers from 300 mb to 30 mb, and 5 km layers from 30 mb to 1 mb, and moisture profiles can be obtained with an accuracy better than 20% absolute errors in 1 km layers from the surface to nearly 200 mb.

RETRIEVAL OF ATMOSPHERIC AND SURFACE PARAMETERS FROM AIRS/AMSU/HSB DATA UNDER CLOUDY CONDITIONS

Joel Susskind[1], Chris Barnet[2], and John Blaisdell[3]

1. *NASA/GSFC, Code 910.4, Greenbelt, MD 20771*
2. *Joint Center for Earth Systems Technology, NASA/GSFC, Code 910.4, Greenbelt, MD 20771*
3. *Science Applications International Corporation, NASA/GSFC, Code 910.4, Greenbelt, MD 20771*

ABSTRACT

New state of the art methodology is described to analyze AIRS/AMSU/HSB data in the presence of multiple cloud formations. The methodology forms the basis for the AIRS Science Team algorithm which will be used to analyze AIRS/AMSU/HSB data on EOS Aqua. The cloud clearing methodology requires no knowledge of the spectral properties of the clouds. The basic retrieval methodology is general and extracts the maximum information from the radiances, consistent with the channel noise covariance matrix. The retrieval methodology minimizes the dependence of the solution on the first guess field and the first guess error characteristics. Results are shown for AIRS Science Team simulation studies with multiple cloud formations. These simulation studies imply that clear column radiances can be reconstructed under partial cloud cover with an accuracy comparable to single spot channel noise in the temperature and water vapor sounding regions, temperature soundings can be produced under partial cloud cover with RMS errors on the order of, or better than, 1°K in 1 km thick layers from the surface to 700 mb, 1 km layers from 700 mb to 300 mb, 3 km layers from 300 mb to 30 mb, and 5 km layers from 30 mb to 1 mb, and moisture profiles can be obtained with an accuracy better than 20% absolute errors in 1 km layers from the surface to nearly 200 mb.

1. INTRODUCTION

AIRS (Atmospheric Infrared Sounder) is a high spectral resolution ($\nu/\Delta\nu \approx 1200$) infrared sounder, with 2378 channels covering the spectral domain 650 cm^{-1} - 2675 cm^{-1}, which will fly on the EOS Aqua platform in 2002, accompanied by the AMSU A (Advanced Microwave Sounding Unit A) and HSB (Humidity Sounder for Brazil, which is similar to AMSU B). The AIRS footprint is 13 km at nadir, as is the HSB footprint, with a 3x3 array of AIRS and HSB footprints falling into a single AMSU A footprint. Characteristics of the AIRS instrument are given in Aumann et al., 2002.

Susskind et al., 1998 described the first version of the methodology used by the AIRS Science team to analyze AIRS/AMSU/HSB data in the presence of clouds to determine surface skin temperature, surface spectral emissivity and bi-directional reflectance, atmospheric temperature-moisture-ozone profile, and the heights and amounts of different layers of clouds in the fields of view. Two important characteristics of the basic retrieval methodology are that no assumptions are needed about the spectral properties of the clouds and no assumptions are needed about the intrinsic accuracy of the first guess field used to start the iterative process. This paper describes further theoretical improvements in the retrieval and cloud clearing methodology incorporated in the current version of the AIRS Science team algorithm which will be used to analyze AIRS/AMSU/HSB data on the EOS Aqua platform. The following sections will describe the basic methodology used to estimate cloud cleared AIRS radiances, which are subsequently used to retrieve surface and atmospheric geophysical parameters other than cloud parameters as well as to derive the effects of clouds on the channel noise covariance matrix; describe the inversion methodology, which makes strong use of the channel noise covariance matrix and is applicable to solving for all the geophysical parameters including cloud parameters; and show sample results from AIRS Science Team simulations.

2. CLOUD CLEARING METHODOLOGY

Clouds have a significant effect on observed infra-red radiances, and can have smaller but non negligible effects on microwave observations as well. Therefore, an accurate treatment of the effects of clouds on the observed AIRS radiances is critical to obtaining accurate soundings. There are three basic approaches for treating cloud effects on the IR observations: look for clear spots and therefore avoid the problem; attempt to solve for the radiative effects of clouds directly in the inversion process; and attempt to infer what the radiances in the clear portions of the scene would be, called clear column radiances, from observations in a number of adjacent fields of view. An example of the first approach is given by Cuomo et al. (1993). Eyre (1989a, 1990) has used the second approach in simulation by assuming an unknown homogeneous amount of black clouds at an unknown pressure, and attempted it with real TOVS data as well (Eyre, 1989b). Our approach, like that used in Susskind et al. (1997), is of the third type and is an extension of that used by Smith (1968), and Chahine (1974, 1977). The advantage of this approach is that it does not have the clear sky sampling bias of the first approach, nor does it require the ability to accurately model the spectral emissive, reflective, and transmissive properties of the clouds, and their dependence on the vertical microphysics and geometry, as required by the second approach. The key assumption made in the third approach is that while there may be many types of clouds in the different fields of view, the radiative properties of a given type of cloud are identical in all fields of view, which differ only in the relative amounts of these cloud types. Fields of view containing clouds with the same optical properties but at different heights, or clouds at the same height but with different optical properties, can be considered as having multiple cloud types. The other key assumption of this approach is that the fields of view have the same characteristics in the clear portions of their scenes, with unknown temperatures, humidities, etc. that we are trying to solve for. We have used analogous assumptions in analyzing 22 years of TOVS data on board the NOAA operational satellites (Susskind et al., 1997) and shown that retrieval accuracy does not degrade appreciably with increasing cloud cover (Chahine and Susskind, 1989). Analogous assumptions are made by NOAA/NESDIS in production of their clear column radiances used in generation of operational HIRS2/MSU retrievals (McMillin and Dean, 1982).

Using these assumptions, Chahine (1977) has shown that in the case of K-1 cloud formations, observations in K fields of view are needed to obtain channel i clear column radiances $\hat{R}_i$ according to

$$\hat{R}_i = R_{i,1} + \sum_{k=1}^{K-1} \eta_k \left(R_{i,1} - R_{i,K+1-k} \right) \qquad (1)$$

where $R_{i,k}$ is the channel i observation in field of view k. We have found it is advantageous (as suggested by L. McMillin) to extrapolate the radiances in the K fields of view according to a similar equation of the form

$$\hat{R}_i = R_{i,AVG} + \sum_{k=1}^{K} \eta_k (R_{i,AVG} - R_{i,k}) \qquad (2)$$

where $R_{i,AVG}$ is the average radiance of all fields of view. Optimal values of η_k will give true values of $\hat{R}_i$ up to instrumental noise effects.

Cloud formations should be distinguished from cloud types. For example, if three fields of view are considered, and two cloud types exist, with cloud top pressures at 300 mb and 700 mb, and the respective cloud fractions as seen from above are (10%, 20%), (20%, 40%), and (30%, 60%) in each field of view, then only a single cloud formation exists with cloud fractions of 30%, 60%, and 90% in each field of view respectively. If instead, the third field of view had cloud fractions of 30% and 65%, then 5% of a second cloud formation exists in the third field of view only. The above discussion applies only to cases in which the upper cloud type is opaque, and a portion of the scene, as observed from above, corresponds to cloud type 1, cloud type 2, or the surface. If the upper cloud type is semi-transparent, then a portion of the scene can correspond to cloud type 1 overlaying the surface, cloud type 1 overlaying cloud type 2, cloud type 2, and the surface. In such a case, three cloud formations will exist in general even if the relative amounts of each cloud type are as initially stated above.

The methodology we use to determine η_k is general for handling up to K-1 cloud formations. The simulations done by the AIRS Science Team, and shown in this paper, used essentially two cloud formations of gray clouds with differing amounts of clouds at 2 discrete levels in each of the 9 AIRS footprints within an AMSU A footprint. The cloud spectral emissivities and cloud top pressures were allowed to vary slightly between fields of view, however. Surface skin properties also had some variability between fields of view. This allows for multiple degrees of freedom within the 3x3 array of AIRS spots in a single AMSU A footprint.

Susskind et al. (1998) used the 9 AIRS spots within an AMSU A footprint to construct 3 fields of view used to determine 2 values of η to be used in Equation 1. Field of view 1 was comprised of the average of the observations in the 3 warmest spots in an 8 μm window channel, and field of view 3 was the average of 3 coldest spots. We now use all radiances in all spots separately and determine 9 values of η. Given η_k, clear column radiances for all channels can be obtained from Equation 2. As in Susskind et al. (1998), we determine the values η and from observations in a selected set of I(= 76) cloud filtering channels which are primarily in between lines in the 15 μm CO_2 band and in the 4.2 μm CO_2 bandhead region, with some additional channels in the window regions. If, for each channel i, one substitutes an estimate of $R_{i,CLR}$ for $\hat{R}_i$ in Equation 2, this gives I equations for K unknowns. The unconstrained weighted least square solution to this multilinear problem is given by

$$\eta_{Kx1} = \left[\Delta R' N^{-1} \Delta R\right]^{-1}_{KxK} \Delta R' N^{-1} \Delta R_{CLR} \quad (3)$$

where ΔR is a IxK matrix with $\Delta R_{i,k} = R_{AVG} - R_{i,k}$, ΔR_{CLR} is an Ix1 matrix given by $\Delta R_{i,CLR} = R_{i,CLR} - R_{i,AVG}$, and N is an IxI channel noise covariance matrix.

The 9 radiances $R_{i,k}$ are observed at 3 different zenith angles. Having observations at different zenith angles will cause additional contributions to ΔR which are not due to differences in cloud cover. To remove these, we adjust all observed channel radiances to what they would have been if taken at the central zenith angle of the 3x3 array of AIRS spots according to Goldberg et al., 2002. From now on, ΔR refers to adjusted observed radiances.

The key to the accurate determination of η is obtaining the best estimates of $\Delta R_{i,CLR}$, along with an accurate treatment of the noise covariance matrix N. As in Susskind et al. (1998), we assume the noise in channel i used to determine η is dominated by errors in $\Delta R_{i,CLR}$. The values of $\Delta R_{i,CLR}$ which we use to determine η (and $\hat{R}_i$) are iterative and are computed based on the current best estimate of all relevant surface and atmospheric properties. For optimal results, it is important for the estimated geophysical parameters to be unbiased over large regions of the atmosphere. For example, if the estimated temperature profile were uniformly too warm, values of $\Delta R_{i,CLR}$ would all be too high and incorrect values of η_k would be obtained which would reconstruct too high values of $\hat{R}_i$. To avoid this, we make sure that the profile used to estimate $R_{i,CLR}$ is consistent with observations in all AMSU A and HSB channels, thus insuring an unbiased temperature and moisture profile over coarse layers in the atmosphere. It would be a mistake to use an analysis or a forecast field directly to compute $R_{i,CLR}$ because this field, while potentially accurate, could be biased in the vertical.

The iterative methodology to determine clear column radiances consists of four passes to determine η^n (n = 1, 2, 3, 4), using four sets of conditions, described later, to estimate $R^n_{i,CLR}$, in which $R^n_{i,CLR}$ and hence η^n, become increasingly more accurate for each iteration. Each set of conditions has its own N^n, reflecting expected errors in $R^n_{i,CLR} - R_{i,1}$. The diagonal term of the noise covariance matrix is modeled according to

$$N^n_{ii} = NE\Delta N_i^2 + \left[\frac{\partial R_i}{\partial T_s}\delta T_s^n\right]^2 + \left[\frac{\partial R_i}{\partial \varepsilon_{\nu_i}}\delta \varepsilon^n_{\nu_i}\right]^2 + \left[\frac{\partial R_i}{\partial \rho_{\nu_i}}\delta \rho^n_{\nu_i}\right]^2 + \left[\frac{\partial R_i}{\partial T(P)}\delta T(P)^n\right]^2 + \left[\frac{\partial R_i}{\frac{\partial q(P)}{q}}\frac{\delta q(P)^n}{q}\right]^2 \quad (4a)$$

and the off diagonal term is given by

$$N^n_{ij} = \frac{\partial R_i}{\partial T_s}\frac{\partial R_j}{\partial T_s}\left(\delta T_s^n\right)^2 + \frac{\partial R_i}{\partial \varepsilon_{\nu_i}}\frac{\partial R_j}{\partial \varepsilon_{\nu_j}}\left(\delta \varepsilon^n_{\nu_i}\delta \varepsilon^n_{\nu_j}\right) + \ldots. \quad (4b)$$

where $NE\Delta N_i$ is the channel i instrumental noise and the remaining terms are contributions to errors in the computed value $R_{i,CLR}$ resulting from errors in estimated surface skin temperature, surface spectral emissivity, surface spectral bi-directional reflectance of solar radiation, and temperature and moisture profile respectively. The partial derivatives are determined empirically by computing the radiance using the current estimate of each parameter and recomputing it after a small change in that parameter. In Susskind et al. (1998), the uncertainties, such as δT_s^n, are specified so as to be indicative of the expected errors for that parameter in pass n. We now predict these errors on a

profile by profile basis for each pass by propagation of expected sources of error through the retrieval process in a manner to be described later. A principal source of retrieval error arises from errors in the reconstructed clear column radiances. These errors propagate into degraded estimates of all the variables shown in Equation 4.

Selection of Optimal Fields of View

The effects of instrumental noise on the clear column radiances will in general be amplified from single spot noise values because the clear column radiances are expressed as a linear combination of the observations in different fields of view. If there were no other sources of error, the diagonal term of the clear column radiance noise covariance matrix in a given pass in Equation 2 would be

$$\left[\delta\hat{R}\cdot\delta\hat{R}'\right]_{ii} = NE\Delta N_i^2\cdot A(\eta_k)^2 \qquad (5)$$

where $A(\eta_k)$ is the noise amplification factor, given by

$$A(\eta_k) = \left[\sum_{k=1}^{9}\left(\frac{1}{9}\cdot\left(1+\sum_{k'=1}^{9}\eta_{k'}\right)-\eta_k\right)^2\right]^{1/2}. \qquad (6)$$

$A(\eta_k)$ is approximately equal to $\left[\Sigma\eta_k{}^2\right]^{1/2}$ because the first term, containing the factor 1/9, is small. It is desirable to find an accurate expression for clear column radiance which minimizes $A(\eta_k)$. We can minimize $A(\eta_k)$ by expressing Equation 2 in terms of radiances in an optimal set of fields of view, given by linear combinations of the original set. The optimal $A(\eta_k)$ can be found by transforming the original contrast fields, to a new set, ΔR_k^T, according to

$$\Delta R_{i,k}^T \equiv \sum_{k'} U_{k,k'}\cdot\Delta R_{i,k'} \qquad (7)$$

where U is the unitary transformation which diagonalizes $\Delta R'\cdot N^{-1}\cdot\Delta R$

$$\left[U'\cdot\left(\Delta R'\cdot N^{-1}\cdot\Delta R\right)U\right]_{k,k'} = \lambda_k\cdot\delta_{k,k'}. \qquad (8)$$

This is equivalent to having selected

$$R_k^T = R_{AVG} - \sum_{k'} U_{k,k'}\left(R_{AVG} - R_{k'}\right). \qquad (9)$$

One eigenvalue λ_k is always zero because only 8 linearly independent values of $\Delta R_{i,k}$ exist. In transformed space,

$$\hat{R}_i = R_{i,AVG} + \sum_{k=1}^{K_{max}}\zeta_k\cdot\Delta R_{i,k}^T \qquad (10)$$

and the solution for ζ_k is given by

$$\zeta_k = \lambda_k^{-1}\cdot\left(\Delta R^{T'}\cdot N^{-1}\cdot\Delta R_{CLR}\right) \qquad (11)$$

where $\Delta R_{i,k}^{T'}$ is the transpose of $\Delta R_{i,k}^T$.

It is apparent that large eigenvalues λ_k imply low values of ζ_k while small eigenvalues imply large (and undesirable) values of ζ_k. The eigenvalues themselves indicate the degrees of freedom in the radiances in the different fields of view corresponding to the different number of cloud formations. Typical cloud formation eigenvalues are the order of 1000. We discard all eigenvalues less than 25 and set K_{max} accordingly, with the constraint that K_{max} is never greater than 4. We also do not include any eigenfunction whose eigenvalue is less than the uncertainty in ζ_k, given later in Equation 13. This reduces the noise amplification factor by suppressing noise in the solution of $\eta_k = \sum_{k'=1}^{K_{max}} U_{k,k'}\cdot\zeta_{k'}$, resulting in lower values of η.

Under certain pathological conditions, one or more cloud formations may not result in significant eigenvalues of $\Delta R'N^{-1}\Delta R$ and cannot be solved for, resulting in a poor solution. The most obvious example of this is a single cloud formation with a constant cloud fraction in each field of view. Here ΔR is comprised of noise only. The most common examples of this are all fields of view are clear, which is a benign case, or all fields of view are overcast, which is a case which must be otherwise identified and rejected. Likewise, with two cloud formations, if the lower cloud deck is overcast, a proper resonstruction of the clear column radiances cannot be obtained. In this case, if the cloud fraction of the upper cloud in fields of view k is α_{1k}, then the lower cloud fraction as seen from above, α_{2k}, is $1-\alpha_{1k}$. In general, if $\alpha_{2k} = A + B\alpha_{1k}$ for all k, then cloud formation 2 will have a zero eigenvalue of $\Delta R'N^{-1}\Delta R$ up to noise effects. The benign case occurs when A=0, corresponding to a truly single cloud formation.

Contribution of clouds to the retrieval channel noise covariance matrix M

The basic retrieval methodology described in the next section requires a channel noise covariance matrix M representing channel correlated errors in the terms $\left(\hat{R}_i - R_i^m\right)$ and $\left(\hat{R}_j - R_j^m\right)$ where R_i^m is the radiance computed for channel i based on the m^{th} iterative solution. The channel noise covariance matrix is the sum of two parts, resulting from noise in the reconstructed clear column radiances $\delta\hat{R}_i$ with noise covariance $\hat{M}$, and noise in the computed radiances δR_i^m due to uncertainty in the parameters assumed known, with noise covariance $\tilde{M}$.

$\hat{M}_{ij} = \left[\delta\hat{R}\delta\hat{R}'\right]_{ij}$ is the expected noise covariance matrix for the channel clear column radiances. The noise in $\hat{R}_i$ obtained from Equation 2 has two parts, arising from instrumental noise $NE\Delta N_i$, and from cloud clearing errors coming from errors in ζ_k. Errors in ζ_k will cause channel correlated clear column radiance errors. Clear column radiances for those channels affected by clouds will have this additional error due to errors in ζ. For the AIRS instrument, the channel noise is spectrally uncorrelated, giving the final result

$$\left[\delta\hat{R}\,\delta\hat{R}'\right]_{ii} = NE\Delta N_i^2\, A(\eta_k)^2 + \left[\Delta R^T \delta\zeta\,\delta\zeta'\Delta R^{T'}\right]_{ii} \quad (12a)$$

and

$$\left[\delta\hat{R}\delta\hat{R}'\right]_{ij} = \left[\Delta R^T \delta\zeta\,\delta\zeta'\Delta R^{T'}\right]_{ij} \quad (12b)$$

where $\delta\zeta\,\delta\zeta'$ is the error covariance of ζ. If N, as defined in Equation 4, is indeed representative of the noise in the determination of η, then it can be shown (see Equation 38) that

$$\left[\delta\zeta\,\delta\zeta'\right]_{kk'} = \left[\Delta R^{T'} N^{-1} \Delta R^T\right]^{-1} = \lambda_k^{-1}\delta_{kk'}. \quad (13)$$

In the special case for which we determine that channel i does not "see" the clouds (i.e., stratospheric sounding channels or tropospheric sounding channels peaking significantly above the highest cloud top), the clear column radiance is best described as the average radiance in all fields of view. For these channels, the scene appears to be clear and we can define effective values of η^{CLR} for "clear" channels as $\eta_k{}^{CLR} = 0$ for all k. For these channels (see Equation 6),

$$A\left(\eta_k^{CLR}\right) = \frac{1}{3} \quad (14)$$

which is a noise reducer. For "clear" channel i, one can write

$$\hat{M}_{ij} = \frac{1}{9} NE\Delta N_i^2\, \delta_{ij} \quad (15)$$

where j is any other channel and δ_{ij} is the Kronecker delta function.

For a channel to be determined not to see clouds, it must be included in a list showing a 95% probability of not seeing a cloud, which is pre-computed as a function of cloud top pressure and zenith angle. In addition, the standard deviation of the radiances in the 3x3 array of AIRS spots must be less than twice the channel noise.

For channels which see clouds, the clear column noise covariance can now be expressed as

$$\hat{M}_{ij} = NE\Delta N_i\, NE\Delta N_j\, A(\eta_k)^2\delta_{ij} + \sum_{k=1}^{K_{max}} \left(\Delta R_{ik}^T \Delta R_{jk}^T \lambda_k^{-1}\right). \quad (16)$$

Errors in clear column radiances can be larger than predicted by Equation 16, however, because λ_k^{-1} is just an estimate of $(\delta\zeta\,\delta\zeta')_{kk'}$. Moreover, Equation 16 does not take into account contributions to the noise covariance matrix arising from higher components of ζ not solved for ($k > K_{max}$) as well as fitting errors due to a poor first guess. Another estimate of the error in the ζ parameters can be computed using weighted radiance residuals in the channels used in the cloud clearing retrieval, $R_{i,CLR} - \hat{R}_i$. If we take $R_{i,CLR} - \hat{R}_i$ as the uncertainty of $\Delta R_{i,CLR}$, then using Equation 11, we estimate the uncertainty in ζ_k according to

$$\left[\delta\hat{\zeta}\,\delta\hat{\zeta}'\right]_{kk} = \left(\frac{1}{\lambda_k}\right)^2 \sum_i \left(\Delta R_{k,i}^T N_{ii}^{-1}\right)^2 \left(R_{i,CLR} - \hat{R}_i\right)^2 \quad (17)$$

which we evaluate for all significant functions k with $\lambda_k > 10^{-3}$. This includes eigen functions with λ_k < 25 and therefore not included in the solution for $\hat{R}_i$. For values of $k \le K_{max}$, we take

$$\left[\delta\zeta\,\delta\zeta'\right]_{kk} = MAX\left[\lambda_k^{-1}, \left[\delta\hat{\zeta}\,\delta\hat{\zeta}'\right]_{kk}\right] \quad (18)$$

and for values of k between K_{max} and K_{sig} (significant eigenvalues $\lambda_k > 10^{-3}$) we set

$$[\delta\zeta\delta\zeta']_{kk} = \left[\delta\hat{\zeta}\,\delta\hat{\zeta}'\right]_{kk} \qquad (19)$$

and write

$$\hat{M}_{ij} = NE\Delta N_i\, NE\Delta N_j\, A(\eta_k)^2\,\delta_{ij} + \sum_{k=1}^{K_{sig}} \Delta R_{ik}^T\, \Delta R_{jk}^T\, [\delta\zeta\delta\zeta']_{kk} \qquad (20)$$

One can think of Equation 20 in terms of a different effective noise amplification factor $A_{i,eff}$ for each channel i

$$\hat{M}_{ii} = NE\Delta N_i^2\, A^2_{i,eff} \qquad (21)$$

where

$$A_{i,eff} = \left[A(\eta_k)^2 + \sum_{k=1}^{k_{sig}} \frac{\Delta R_{i,k}^{T^2} [\delta\zeta\delta\zeta']_{kk}}{NE\Delta N_i^2} \right]^{1/2} . \qquad (22)$$

The channel effective noise amplification factor is largest for channels which see the surface and have potentially large values of the scene contrast $\Delta R_{i,k}$. We find it convenient to define an effective noise amplification factor relevant to the surface channel retrieval step as the RMS value of $A_{i,eff}$ over all NSURF infrared channels used in the surface retrieval step

$$A_{eff} = \frac{1}{NSURF}\left[\sum_{i=1}^{NSURF} A_{i,eff}^2 \right]^{1/2} . \qquad (23)$$

Very large values of A_{eff} can arise when $\delta\zeta\delta\zeta'$ is large (A_{eff} is sometimes 100 or more) and indicate a large uncertainty in the determination of the clear column radiances. These large uncertainties are sometimes caused by hidden, or nearly hidden cloud formations, and often correlate with poor solutions.

3. BASIC RETRIEVAL METHODOLOGY

The basic retrieval methodology is the same as that of Susskind et al. (1998) and is reviewed below. After a start up procedure to determine the clear column radiances, we use AIRS/AMSU/HSB data to retrieve:
a) surface skin temperature, surface spectral emissivity and surface bi-directional reflectance of solar radiation; b) atmospheric temperature profile; c) atmospheric moisture profile; d) atmospheric ozone profile; and e) cloud properties. These steps are done sequentially, solving only for the variables to be determined in each step and using previously determined variables as fixed but with an appropriate uncertainty attached to them which is accounted for in the channel noise covariance matrix M. The objective in each step is to find solutions which best match the observations for a select set of channels, bearing in mind the channel noise estimates. The "observations" in steps a-d are the clear column radiances as determined from Equations 10 and 11, with values of ζ^{CLR} used for appropriate channels. The cloud parameters determined from step e are found so as to be most consistent with the actual observed radiances and the clear sky geophysical parameters determined from steps a-d. Steps a-d are ordered so as to allow for selection of channels in each step which are primarily sensitive to variables to be determined in that step or determined in a previous step, and relatively insensitive to other parameters. Separation of the problem in this manner also allows for the problem in each step to be made as linear as possible. Steps a-e are all solved for in a completely analogous manner, linearizing the problem about initial guess parameters and iterating the solution until convergence is reached. In general, these linear equations are ill conditioned and require some form of stabilization, which is commonly based on an estimate of the accuracy of the *a-priori* information obtained in the first guess or background field (Rodgers, 1976; Hanel et al., 1992). The methodology we have developed, described in the next section, relies exclusively on the signal to noise of the observations to indicate the degree to which the information contained in the radiances should be believed, and does not involve use of an estimate of the accuracy of the background field.

Iterative least squares solution to the non-linear problem

The solution to each of the five steps described above is done in the form

$$X^m = X^{m-1} + \sum_{\ell=1}^{L} F_\ell\, \Delta A_\ell^m = X^0 + \sum_{\ell=1}^{L} F_\ell\, A_\ell^m \qquad (24)$$

where X^m is the m^{th} iterative state, F_ℓ is a set of L functions, and

$$A_\ell^m = A_\ell^{m-1} + \Delta A_\ell^m . \qquad (25)$$

ΔA_ℓ^m is determined each iteration so as to minimize the residuals $\Delta\Theta^m$, weighted inversely with respect to expected noise levels, for the channels used to determine A_ℓ. The residual for channel I is defined as

$$\Delta\Theta_i^m = \left(\hat{R}_i - R_i^m\right)\left(\frac{dB_i}{dT}\right)^{-1}_{\Theta_i^m} \qquad (26)$$

where $\hat{R}_i$ is the reconstructed clear column radiance, R_i^m is the radiance computed from the m^{th} iterative parameters, and Θ_i^m is the brightness temperature corresponding to R_i^m. The m^{th} iterative residual for channel i is attributed to errors in the coefficients δA^m and to the noise effects,

$$\Delta\Theta_i^m = \sum_\ell S_{i\ell}\,\delta A_\ell^m + \tilde{\Theta}_i, \qquad (27)$$

where $S_{i\ell}$ is an element of the sensitivity matrix, or Jacobian, given by

$$S_{i\ell}^m = \frac{\partial R_i^m}{\partial A_\ell}\left(\frac{dB_i}{dT}\right)^{-1}_{\Theta_i^m} \qquad (28)$$

and the noise factor $\tilde{\Theta}_i$ for a given case has two parts: errors in observed clear column radiance $\delta\hat{\Theta}_i$ which are affected by instrumental noise and cloud clearing errors, and computational noise $\delta\Theta_i^c$.

In the simulations done thus far, we have assumed perfect knowledge of physics, i.e., if we know all of the variables exactly, we can compute exact noise free radiances. Nevertheless, the transmittances depend on the variables to be solved for. Therefore, computational noise exists. Computational noise, arising from errors such as a low (high) estimate of atmospheric water vapor, will produce noise that is spectrally correlated. Instrumental noise is spectrally uncorrelated but cloud cleared radiance errors are correlated. Each retrieval step in pass n uses an appropriate noise covariance matrix

$$M_{ij} = \left(\hat{M}_{ij}^n + \tilde{M}_{ij}\right)\left(\frac{dB_i}{dT}\right)^{-1}_{\Theta_i}\left(\frac{dB_j}{dT}\right)^{-1}_{\Theta_j} \qquad (29)$$

where $\hat{M}$ was defined in Equation 20.

The matrix $\tilde{M}$ in Equation 29 represents channel correlated uncertainties in the computed radiances R_i^m and R_j^m based primarily on uncertainties in the parameters being held fixed in a given retrieval step. For example, when we are solving for temperature profile, we are holding fixed surface parameters, moisture profile, and ozone profile. We currently write

$$\tilde{M}_{ii} = 0.1^2\left(\frac{\partial B_i}{\partial T}\right)^2_{\Theta_i} + \left(\frac{\partial R_i}{\partial T_s}\delta T_s\right)^2 + \left(\frac{\partial R_i}{\partial \varepsilon_{v_i}}\delta\varepsilon_{v_i}\right)^2 + \left(\frac{\partial R_i}{\partial \rho_{v_i}}\delta\rho_{v_i}\right)^2 + \left(\frac{\frac{\partial R_i}{\partial q(P)}\frac{\delta q(P)}{q}}{q}\right)^2 + \left(\frac{\frac{\partial R_i}{\partial O_3(P)}\frac{\delta O_3(P)}{O_3}}{O_3}\right)^2 \qquad (30a)$$

and

$$\tilde{M}_{ij} = \left[\left(\frac{\partial R_i}{\partial T_s}\right)\left(\frac{\partial R_j}{\partial T_s}\right)\delta T_s^2 + \ldots\right]. \qquad (30b)$$

The terms in Equations 30a and 30b do not depend to first order on the variables being solved for or the iterative state m. The term 0.1^2 included in Equation 30a is taken to represent additional uncertainties in computed brightness temperatures based on the imperfect knowledge of the variables being solved for, as well as potential spectroscopic errors. The methodology used to predict and propagate errors such as δT_s for use in the computation of $\tilde{M}$ will be discussed later. These terms are analogous to the terms in Equation 4, but uncertainty in O_3 profile was not included in Equation 4 as it did not prove to have a significant effect on the solution and the calculation is computationally expensive.

Application of a constraint H

The standard constrained solution (Hanel et al., 1992) to this problem is given by

$$\Delta A^m = \left[S^{m'} M^{-1} S^m + H^m\right]^1 S^{m'} M^{-1}\,\Delta\Theta^m \qquad (31)$$
$$= D^m \Delta\Theta^m$$

where H^m is a stabilization matrix. Without stabilization, $S\Delta A$ would minimize the weighted residuals $\Delta\Theta' M^{-1}\Delta\Theta$, but the matrix elements of D might be large. This is undesirable as it amplifies errors in $\Delta\Theta^m$ in determining ΔA^m. The key to optimization of the solution lies in accurate treatment of the terms

$\Delta\Theta$, S and M; a judicious choice of the functions F and channels i; and optimal treatment of the constraint matrix H. Hanel et al. (1992) and Rodgers (1976) have reviewed several methods of constraining the ill-conditioned inverse problem. In the minimum variance approach (Rodgers, 1976), H is taken to be the inverse of the *a priori* error covariance. If the statistics of both the measurement and *a priori* are Gaussian, the maximum likelihood solution is obtained. If the *a priori* covariance is taken to be $H = \gamma I$, the maximum entropy solution is obtained. Other forms of H include the first or second derivative formulations (Twomey, 1963) that force a smoothness constraint on the solution. The solution can also be constrained by the relaxation method (Chahine, 1968) and by the Backus and Gilbert (1970) method.

The minimum variance and maximum likelihood solutions are often considered to be "optimal." However, if the *a priori* error covariance is not known or estimated incorrectly, the solution will be sub-optimal. If the *a priori* errors are underestimated, the solution could be overconstrained. This could potentially create biases in the retrievals. The biases may mask small trends in the retrieved data that one may be trying to extract. The approach described here attempts to keep the effects of instrument noise at a tolerable level without assumptions regarding the *a priori* data error covariance.

Our objective is to determine a constraint matrix that affects only the pieces of information not well determined by the radiances. This involves use of an optimal set of functions G, related to F by a unitary transformation

$$G = FU \tag{32}$$

in terms of which we could write

$$X^m = X^{m-1} + G\Delta B^m = X^{m-1} + FU\Delta B^m = X^{m-1} + F\Delta A^m \ . \tag{33}$$

In terms of the functions G, Equation 31 becomes

$$\Delta B^m = U'\Delta A^m = \left(U^{m'}S^{m'}M^{-1}S^mU^m + H^m\right)^{-1} \cdot U^{m'}S^{m'}M^{-1}\left(\Delta\Theta^m - \delta\Theta^{m-1}\right). \tag{34}$$

A new term $\delta\Theta^{m-1}$ has been included in Equation 34 which is a background correction term that is zero in the first iteration and will be discussed in detail later. The optimal transformation matrix U^m is chosen so that $U^{m'}S^{m'}M^{-1}S^mU^m$ is diagonal with eigenvalues λ_ℓ. The inverse of each eigenvalue is the variance of eigenmode G_ℓ. The unconstrained solution, with both $H_{ij} = 0$ and with no background correction $\left(\delta\Theta^n = 0\right)$, is given by

$$\Delta B_\ell^m(0) = \left(\lambda_\ell^m\right)^{-1}\left(U^{m'}S^{m'}M^{-1}\right)_\ell \Delta\Theta^m = \left(\lambda_\ell^m\right)^{-1} d_\ell^m \Delta\Theta^m \tag{35}$$

where d_ℓ^m is the ℓ^{th} row of $U^{m'}S^{m'}M^{-1}$. Low values of λ_ℓ, indicating ill-conditioned variables G_ℓ, would lead to large coefficients of $\Delta\Theta^n$ in the determination of ΔB_ℓ^m if the solution for the coefficients of these functions were unconstrained. We therefore only constrain the solution of those functions G_ℓ with low eigenvalues and set $H_{\ell\ell'}^m = \Delta\lambda_\ell^m\,\delta_{\ell\ell'}$. The constrained solution is now given by

$$\Delta B_\ell^m\left(\Delta\lambda_\ell^m\right) = \frac{\lambda_\ell^m}{\lambda_\ell^m + \Delta\lambda_\ell^m}\Delta B_\ell^m(0) = \Phi_\ell^m\,\Delta B_\ell^m(0) \tag{36}$$

where Φ is a damping factor equal to unity if no constraint is applied and zero if $\Delta\lambda_\ell$ is infinite. If $\Phi_\ell = 1$, all the information about G_ℓ obtained from the radiances is believed. Otherwise only Φ_ℓ of the information in the radiances is believed, and $(1-\Phi_\ell)$ of the *a-priori* information is believed.

The objective of damping a mode is to reduce propagation of noise $\delta\tilde{B}_\ell(\Delta\lambda_\ell)$ which is given by

$$\delta\tilde{B}_\ell^m\left(\Delta\lambda_\ell^m\right) = \left(\lambda_\ell^m + \Delta\lambda_\ell^m\right)^{-1}\left(U^{m'}S^{m'}M^{-1}\right)_\ell\delta\tilde{\Theta}^m \tag{37}$$

where $\delta\tilde{\Theta}^m$ is the noise in $\Delta\Theta_i$. A statistical estimate of $\delta\tilde{B}_\ell^m$ over an ensemble of profiles is given by

$$\delta\overline{B}_\ell(\Delta_\lambda) = \left[\delta\tilde{B}^m\,\delta\tilde{B}'^m\right]_{\ell\ell}^{1/2} = \left(\lambda_\ell^m + \Delta\lambda_\ell^m\right)^{-1} \cdot \left[U^{m'}S^{m'}M^{-1}\delta\tilde{\Theta}\delta\tilde{\Theta}'M^{-1}S^mU^m\right]_{\ell\ell}^{1/2} = \frac{\left(\lambda_\ell^m\right)^{1/2}}{\lambda_\ell^m + \Delta\lambda_\ell^m} = \Phi_\ell\cdot\left(\lambda_\ell^m\right)^{-1/2} \tag{38}$$

to the extent that M accurately represents $\delta\tilde{\Theta}\delta\tilde{\Theta}'$, the noise covariance of $\Delta\Theta$. We assign a noise propagation threshold ΔB_{max} for each type of retrieval (surface properties, temperature profile, etc.) and set $\Delta\lambda_\ell = 0$ if $\delta\overline{B}_\ell(0) \le \Delta B_{max}$. Otherwise, we obtain $\Delta\lambda_\ell$ such that $\delta\overline{B}_\ell(\Delta\lambda_\ell) = \Delta B_{max}$.

Formulation of the background term

The need for an iterative process arises because the radiative transfer equation is not linear. In every iteration, we recompute Θ_i^m, as well as S^m, U^m and λ^m. If the solutions were completely linear, and we applied no damping, then

$$\Delta\Theta^{m+1}(0) \equiv \hat{\Theta} - \Theta^{m+1}(0) \cong \Delta\Theta^m - S^m U^m \Delta B^m(0) \quad (39)$$

and $\Delta B^{m+1}(0)$ would be determined to be zero because $\Delta B^m(0)$ would have already minimized the residuals $\Delta\Theta^m$.

The residual $\Delta\Theta^{m+1}$ is not zero however, both because $\Theta^{m+1}(0)$ is not given exactly by $\Theta^m + S^m U^m \Delta B^m(0)$ as a result of non-linearity, and because $\Delta B_\ell^m \neq \Delta B_\ell^m(0)$. As a result of applying ΔB_ℓ^m rather than $\Delta B_\ell^m(0)$, we obtain

$$\Delta\Theta^{m+1} \approx \Delta\Theta^{m+1}(0) + S^m U^m \left[\Delta B^m(0) - \Delta B^m\right] = \Delta\Theta^{m+1}(0) + \delta\Theta^m \quad (40)$$

In Equation 40, $\Delta\Theta_\ell^{m+1}(0)$ represents the portion of $\Delta\Theta^{m+1}$ that is due to effects of non-linearity on the solution, while $\delta\Theta^m$ represents the residual portion of $\Delta\Theta^{m+1}$ due to the effects of damping in iteration m. The second term is zero for undamped modes and increases in significance with increased damping. This term is also zero for all modes in the first iteration. We only want to include the effects of non-linearity on $\Delta\Theta^m$ in the iterative procedure used in the determination of ΔB^m. Therefore, the background term to be used in Equation 34 is given by

$$\delta\Theta^{m-1} = S^{m-1} U^{m-1} \left[\Delta B^{m-1}(0) - \Delta B^{m-1}\right] \quad (41)$$

and we solve for ΔB_ℓ^m according to

$$\Delta B_\ell^m = \left(\lambda_\ell^m + \Delta\lambda_\ell^m\right)^{-1} U^{m'} S^{m'} M^{-1} \cdot \left[\Delta\Theta^m - \delta\Theta^{m-1}\right] = \Phi^m \Delta B_\ell^m(0) - \left(\lambda_\ell^m + \Delta\lambda_\ell^m\right)^{-1} \cdot \left[U^{m'} S^{m'} M^{-1} S^{m-1} U^{m-1} \left(\Delta B_\ell^{m-1}(0) - \Delta B_\ell^{m-1}\right)\right] \quad (42)$$

where ΔB_ℓ^{m-1} is the value of ΔB_ℓ which was applied in iteration m-1. Inclusion of the background term in Equation 42 insures second order convergence along the lines discussed by Rodgers (1976) with regard to treatment of the *a-priori* term.

Convergence Criteria

In solving Equation 42, we are attempting to find solutions to the radiative transfer equations which minimize weighted residuals of observed and computed brightness temperatures, corrected for the background term. To test convergence of the solution, one should monitor the weighted residual

$$R = \left[(\Delta\Theta - \delta\Theta)' V' V (\Delta\Theta - \delta\Theta) \right]^{1/2}, \quad (43)$$

where the weight matrix V accounts for noise effects on the channel residuals, as well as the relative information content of the channels with regard to the variables being solved for. For example, if a channel (or linear combination of channels) carries little information content in terms of signal to noise, it should be given little weight in the estimation of the residual in Equation 43. An appropriate choice of V, expressing the information content of the channels, would therefore be $V = \left(\lambda_\ell + \Delta\lambda_\ell\right)^{-1} \left(U'S'M^{-1}\right)$, in which case we obtain

$$R = \left[\Delta B' \Delta B\right]^{1/2}. \quad (44)$$

As shown in Equation 44, a reasonable way to determine if the solution has converged, in terms of weighted residuals of observed minus computed brightness temperatures, is to see if the solution has converged in terms of the iterative changes in the solution itself. Initially, we set $\Delta B_j = 0$ if $\Phi_\ell^1 < 0.05$, that is, coefficients of very heavily damped components with little information content are not believed at all in any iteration. The solution is said to have converged when the RSS value of ΔB_ℓ^m is less than 10% of the RSS value of $\delta\overline{B}^m$ for all components not set equal to

zero. The iterative procedure is also terminated if the RSS value of ΔB_ℓ^m is not less than 75% of that of ΔB_ℓ^{m-1} for the non-zero components. This indicates the solution is not converging rapidly enough and may be responding primarily to unmodeled noise. The iterative procedure, which typically converges by 3 iterations, is carried out analogously for all retrieval steps.

Variables and functions for retrieval steps

As shown in Equation 24, all steps involve expression of the basic variables X in terms of a set of functions F. In the temperature profile retrieval step, the temperature perturbation functions F(P) are 24 trapezoids piecewise linear in log of pressure, spanning the pressure range .016 mb to the surface, with a perturbation of 0.5K between pressures P_ℓ and $P_{\ell-1}$, and 0° at $P_{\ell+1}$ and $P_{\ell-2}$. In the top and bottom functions, the top or bottom portion of the trapezoid is missing. The Jacobian $S_{i\ell}^m$ is obtained numerically by computing the channel i brightness temperature for the m^{th} iterative temperature profile $T^m(P)$ and subtracting it from the brightness temperature computed with everything else fixed but perturbing $T^m(P)$ by one unit of $F_\ell(P)$. With regard to water vapor and ozone profiles, we express solutions in the form

$$q^{m+1}(P) = q^m(P)\left[1 + \sum A_\ell F_\ell(P)\right] \qquad (45)$$

with the functions (L = 11 for water vapor and 8 for ozone) and methodology for computation of the Jacobian being completely analogous to those for temperature profile. In the case of surface variables, the functions are a discrete value of surface skin temperature, as well as 9 triangle functions in the frequency domain dealing with perturbations of surface emissivity and 3 with surface bi-directional reflectance of solar radiation. The total precipitable water also can be adjusted by using Equation 45 with a single function which is constant as a function of height. The window channels are sensitive to boundary layer water vapor but not higher level water vapor. Adjustment of total precipitable water is used in an intermediate retrieval step, done before the water vapor retrieval step using AIRS channels, and improves total low level water vapor at the expense of upper level water vapor. Table 1 shows the pressure levels used in the temperature profile, moisture profile, and ozone profile retrieval steps.

Table 1. Trapezoid Function Endpoints (mb)

Temperature Retrieval	Moisture Retrieval	Ozone Retrieval
0.016	0.016	0.016
0.714	170.1	20.92
1.297	272.9	51.53
2.701	314.1	71.54
4.077	343.6	103.0
8.165	407.5	142.4
16.43	496.6	300.0
23.45	617.5	surface
39.26	706.6	
56.13	852.8	
71.54	surface	
96.11		
125.6		
160.5		
212.0		
272.9		
343.6		
424.5		
496.7		
596.3		
661.2		
753.6		
878.6		
surface		

Selection of channels

While AIRS has 2378 channels, it is neither necessary nor optimal to use all the channels in the retrieval process as the information content of these channels is highly redundant. Therefore, computational time can be lowered by limiting the number of channels used. In a given step, it is preferable to use channels which are primarily sensitive to the variables being solved for, while relatively insensitive to variables not yet solved for. We also find it desirable to use channels with sharp localized weighting functions. Kaplan et al. (1977) show that channels with sharpest weighting functions lie either in between absorption lines or on

the band head of the 4.3 μm CO_2 band between 2378 cm^{-1} and 2390 cm^{-1}. The first set of channels have sharp weighting functions because of a rapid increase of absorption coefficient with increasing pressure, while the second benefit from a rapid increase of absorption coefficient with increasing temperature in the troposphere. Such channels form the basic set used for temperature sounding. Channels in between water vapor absorption lines also produce very sharp weighting functions which are preferable for water vapor sounding and also useful for temperature sounding if the water vapor distribution is known accurately. Channels between absorption features are by definition less opaque than nearby channels situated on absorption features, and may not have sufficient opacity to be sensitive to either temperature or constituents at high enough levels in the atmosphere. For temperature profile, we select channels in the CO_2 Q branch at 667 cm^{-1}, which do not have sharp weighting functions but are sensitive to temperature variations up to 1 mb. We do not select channels in the most opaque portion of the 4.3 μm CO_2 band because these channels are sensitive to effects of non-local thermodynamic equilibrium. For water vapor, we selected a few channels on the peaks of some of the strongest absorption features in the 6.7 μm water vapor band to increase the sensitivity to stratospheric and upper tropospheric water vapor. Window channels are highly redundant with each other and have been selected generally on and off closely lying weak absorption features in the spectral regions from 755 cm^{-1} - 980 cm^{-1}, 1070 cm^{-1} - 1240 cm^{-1}, 2180 cm^{-1} – 2192 cm^{-1}, and 2390 cm^{-1} to 2665 cm^{-1}. Cloud filtering channels are generally a subset of the temperature sounding channels which are sensitive to the troposphere. Our sounding methodology involves two temperature profile retrieval steps, one (temp 1) before the water vapor retrieval step, and the other (temp 2) subsequent to it. In temp 2, we include a number of channels in the water vapor absorption band which produce sharp temperature weighting functions. These channels are treated as "noisy" in the channel noise covariance matrix to the extent that the prediced uncertainty in water vapor distribution produces an appropriate uncertainty in their computed brightness temperatures. The location of all channels used are shown in Figure 1. We use 53 channels in the surface temperature retrieval, 147 channels in the first temperature profile retrieval, an additional 7 channels in the second temperature profile retrieval, 66 channels in the water vapor profile retrieval, and 23 channels in the ozone profile retrieval. Some channels are used for more than one purpose. Channels also exist which can be used for retrievals of profiles of CH_4, CO, and CO_2. These will be described in a future publication.

Table 2 shows the eigenvalues and damping factors for the second pass temperature profile retrieval, the water vapor retrieval, and the ozone profile retrieval for a typical case. Coefficients of eight temperature profile functions are undamped, and those of two more functions are only slightly damped, giving about 9 pieces of information about the temperature profile being contained in the radiances. Roughly 4 1/2 pieces of information about water vapor are contained in the radiances, and roughly 1 1/2 pieces of information are contained about the ozone profile in this case.

Table 2. Sample Eigenvalues and Damping Factors ($\Phi > 0.05$)

Temperature Profile $\Delta B_{max} = 0.75$		Water Vapor Profile $\Delta B_{max} = 1.0$		Ozone Profile $\Delta B_{max} = 0.75$	
λ	Φ	λ	Φ	λ	Φ
94.40	1.0	69.78	1.0	41.59	1.0
65.06	1.0	10.31	1.0	0.745	0.419
36.81	1.0	2.44	1.0	0.403	0.278
26.55	1.0	1.26	1.0	0.139	0.079
12.19	1.0	0.68	0.668		
6.96	1.0	0.27	0.270		
3.84	1.0	0.09	0.095		
1.84	1.0	0.07	0.069		
1.21	0.685				
0.80	0.447				
0.50	0.281				
0.35	0.196				
0.29	0.161				
0.20	0.114				
0.11	0.006				

Cloud parameter retrievals

In performing cloud parameter retrievals, all other variables are assumed known within their estimated

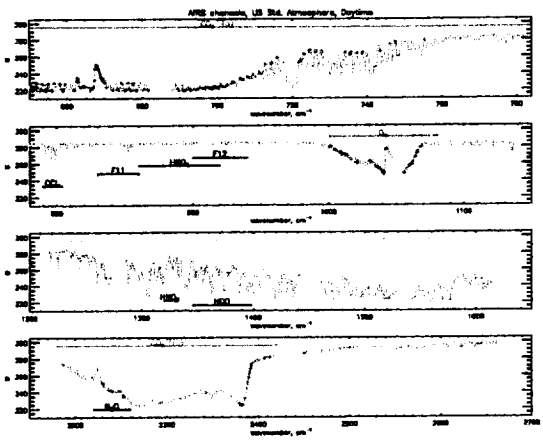

Figure 1. AIRS spectrum showing channels used in different retrieval steps. Temperature sounding channels are red, ozone are green, water vapor are blue, and surface channels are orange.

errors, allowing us to compute $R_{i,CLR}$. The channels used are the subset of cloud clearing channels that are not sensitive to solar radiation reflected off the clouds. The cloud parameter retrieval algorithm is analogous to that of the other steps but slightly different. At this time, the cloud retrieval algorithm has been tested only for the case of assumed cloud spectral properties in order to determine cloud fractions and cloud top pressures for up to two layers of clouds. The method is easily generalizable to include cloud spectral emissivity by inclusion of an appropriate set of spectral emissivity functions as done in the surface parameter retrievals. With known spectral properties, cloud radiances $R_i(P_c)$ can be calculated based on the surface skin temperature and atmospheric temperature-moisture-ozone profile, which have been retrieved from the clear column radiances and are "known", as a function of unknown cloud top pressure P_c. For two cloud layers (the method works for any number of cloud layers) we can write

$$R_{ik} = (1-\alpha_{1k}-\alpha_{2k})R_{i,CLR} + \alpha_{1k}R_i(P_{c1}) + \alpha_{2k}R_i(P_{c2}) \quad (46)$$

where R_{ik} is the radiance computed for channel i in field of view k covered by (as seen from above) α_{1k} fractional coverage of a cloud at P_{c1} and α_{2k} of a cloud at P_{c2}. In the above equation, we have assumed two types of clouds in each of the fields of view k=1,9, with different cloud fractions in each field of view. All clouds were assumed to have a constant spectral emissivity of 0.9. In order to determine the variables $P_{c1}, P_{c2}, \alpha_{11}, \alpha_{12}\ldots$, we use observations in the 9 fields of view for the subset of channels used to determine η which are unaffected by solar radiation. The noise covariance matrix N used to retrieve cloud parameters is identical to that used in Equation 4 to determine η, but for the appropriate subset of channels.

Given the m^{th} guess cloud parameters $\alpha_{1k}^m, \alpha_{2k}^m, P_{c1}^m$, and P_{c2}^m, we define

$$Y_{ik}^m = R_{i,k} - R_{ik}^m = (R_{i,k} - R_{i,CLR}) + \sum_{j=1,2}\alpha_{jk}^m\left(R_{i,CLR} - R_i\left(P_{cj}^m\right)\right) \quad (47)$$

and obtain the iterative equation

$$Y_{ik}^{m+1} - Y_{ik}^m = \sum_{j=1,2}\left[\left(R_{i,CLR} - R_i\left(P_{cj}^m\right)\right)\right]\Delta\alpha_{jk}^m + \sum_{j=1,2}\left[\alpha_{jk}^m\left(\frac{-\partial R_i(P_{cj})}{\partial P_{cj}}\right)\right]\Delta P_{cj}^m = \sum_{j=1,2}\left[S_{ik,\Delta\alpha_{jk}}^m\right]\Delta\alpha_{jk}^m + \sum_{j=1,2}\left[S_{ik,\Delta P_{cj}}^m\right]\Delta P_{cj}^m \quad (48)$$

where the terms in the square brackets are the appropriate Jacobians, which are computed empirically as are all other Jacobians. It should be noted that if α_{jk} (for all k) and/or $\frac{\partial R_i}{\partial P_{cj}}$ (for all i) are small for a given P_{cj}, that cloud top pressure will be contained primarily in a heavily damped mode and not be changed significantly from the initial guess.

Error Propagation and Channel Noise Covariance Matrix

Equations 4 and 30 contain terms such as $\delta T(P)$, indicative of expected errors in state parameters used in a given pass and step. These errors are case dependent and can be estimated by propagating expected errors through the retrieval system. In any iteration, the estimate of a parameter, such as $T(P)^m$, is given by

$$T(P)_j^m = T(P)_j^0 + \sum_{\ell=1}^{L} F_{j\ell}A_\ell^m = T(P)_j^0 + (FUB^m)_{j,1} \quad (49)$$

where j is a discrete pressure level. There are three contributions to the expected error $\delta T(P)_j^m$. The first

contribution comes from the null space error, arising from the error of the first guess in the space outside that of the L functions used to expand the solution. The second component arises from errors in the coefficients B^m. The last contribution arises from the damping of the solution in which $(1-\Phi)$ of the first guess (or previous iteration) is believed for each eigen function G=FU.

Equations 4 and 30 contain the square of the expected error in state parameter X_j^m, $\delta X_j^{m^2}$, which can be expressed in terms of errors in the expansion coefficients A according to

$$\delta X_j^{m^2} = \delta X_j^{N^2} + \sum_k F_{jk}^2 \delta A_k^{m^2} \qquad (50)$$

where δX_j^N is the null space error and δA^m is the error in the coefficients A^m used to represent X^m. Errors in A arise both from errors in the B coefficients and errors in the damped portion of the m-1 iterative guess. In every step in the retrieval process, we begin with parameters X^0 having an uncertainty δX_j^0. The uncertainty of the microwave product first guess is specified based on expected errors, as is the null space error. Given δX^0, δA^0 can be solved for according to

$$\delta A_k^0 = \left[(F'^2 F^2)^{-1} F'^2 \left(\delta X^0 - \delta X^N \right)^2 \right]^{1/2} = \left[\left(F'^2 F^2 \right)^{-1} F'^2 \left(\delta \tilde{X}^0 \right)^2 \right]^{1/2} \qquad (51)$$

In a given iteration, we can express δA_k^m according to

$$\delta A_k^m = \left[\sum_\ell \left(U_{k\ell} \cdot \frac{\Phi_\ell^m}{\sqrt{\lambda_\ell^n}} \right)^2 + \sum_\ell \left(U_{k\ell} (1-\Phi_\ell^m) \sum_j U_{j\ell} \delta A_j^{m-1} \right)^2 + \delta A_k^{N^2} \right]^{1/2} \qquad (52)$$

where $\frac{\Phi_\ell^m}{\sqrt{\lambda_\ell^m}}$ represents the predicted error in B_ℓ^m due to noise propagation, and the second term represents the portions of the errors δB_ℓ^{m-1} of the previous iterative profile which are believed in the current iteration. Given δA_k^m from Equation 52 for the final iterative step, we compute the square of the corresponding profile error to be used in Equations 4 and 30 according to Equation 50. This term is carried to the next retrieval step and used in Equation 51 to give δA_k^0 which is in turn used in Equation 52 to generate the uncertainty in parameter X for use in subsequent steps.

For moisture and ozone profile, the form of the expansion is slightly different (see Equation 45) and we write

$$\left(\frac{\delta q^m(P)}{q} \right)^2 = \left(\frac{\delta q^N(P)}{q} \right)^2 + \sum_k F_k^2(P) \delta A_k^{m^2} \qquad (53)$$

Surface spectral emissivity and bi-directional reflectance are analogous to temperature profile, as is skin temperature, in which case F is a number. The liquid water profile comes from the microwave product and is not iterated. We assume an error estimate of 20% of the liquid water profile. In addition, if the total liquid water is less than 0.01 g/cm^2, we consider the possibility that liquid water may have been missed due to an error in the water vapor microwave solution. For these low liquid water solutions, an alternative error estimate of (2*RH-1)*0.05*q, where RH is the relative humidity and q is the layer water vapor in mg/cm^2, is considered and used if it is larger than 20% of the liquid water. The null space temperature error is taken as 0.1K in the lower and upper atmosphere, increasing to 0.2K near the tropopause. The null space error in percent is taken as 5% for water vapor and 10% for ozone respectively.

Equation 52 is case dependent through the parameters Φ_ℓ and λ_ℓ which depend both on the S matrix, and more significantly on the M matrix. M contains contributions from clouds, $\hat{M}$, and parameter uncertainty $\tilde{M}$. The uncertainties determined from Equations 52, 50, and 53 in turn are used in the computation of $\tilde{M}$ (Equation 30) and N (Equation 4).

Equations 50 and 53 give the magnitude of the estimated error in each parameter but contain no information about sign. If we assume all $\partial X(P)$ are of the same sign, we would overestimate the effect of the uncertainty on that parameter on the computed radiances. Bearing this in mind, when the derivatives in Equations 4 and 30 are computed numerically , we write

$$\frac{\partial R}{\partial X(P)} \partial X(P) = R(X(P) + \Delta X(P)) - R(X(P)) \qquad (54)$$

where $\Delta X(P)$ is constructed by multiplying $\partial X(P)$ by a sine wave with a full period of six temperature profile functions in the case of uncertainty of temperature profile to be used in the humidity and ozone profile retrievals, and six humidity profile functions in the case of water vapor uncertainty to be used in the temperature and ozone profile retrievals. In the case of ozone profile, with only seven functions, we simply multiply the predicted uncertainty by 0.5. We have also found that in constructing the noise covariance terms in Equation 4, it is advantageous to set $\Delta X = 0.5\ \delta(X)$ for all profile terms. For surface parameters we take $\Delta X = \partial X$, as for the liquid water profile.

Steps in the processing system

The processing system used in this paper is comprised of a number of sequential steps listed below. All steps start from the conditions found in the previous step, with appropriate computed uncertainty estimates, δX^0, unless otherwise noted.

1. Use as a starting point the microwave product which agrees with the AMSU A, HSB radiances (Rosenkranz, 2000). We follow this by a temperature profile retrieval using AMSU A radiances as well as AIRS radiances for channels that never see clouds, followed by a water vapor retrieval using HSB channels and some AMSU A window channels. As part of the temperature profile retrieval, we also update the surface skin temperature and microwave spectral emissivity.

2. Determine an initial ζ^1 from Equation 11 using the atmospheric and surface parameters obtained in Step 1. We also perform a cloud parameter retrieval to help determine which IR channels are not affected by clouds. $\hat{R}_i^1$ is obtained using ζ^1 in Equation 10.

3. Determine the first guess IR surface parameters and temperature-moisture-ozone profile using $\hat{R}_i^1$ based on a regression step using most AIRS channels (Goldberg et al., 2002). Under some difficult cloud conditions, this first guess is modified in a manner described later.

4. Produce an improved temperature profile and microwave spectral emissivity starting from the surface and atmospheric parameters determined in step 3 using the AMSU A channel radiances and AIRS channel radiances which do not see clouds. The surface skin temperature is not updated as it is estimated better from AIRS radiances than can be determined from AMSU radiances. This is followed by an improved water vapor profile using HSB radiances.

5. Determine ζ^2 taking advantage of the refined parameters. Also determine cloud parameters to decide which channels do not see clouds so as to average radiances in these channels when producing $\hat{R}_i^2$. $\hat{R}_i^2$ is considerably more accurate than $\hat{R}_i^1$ because the surface and atmospheric parameters obtained from the AIRS regression step are more accurate than those from the microwave first product, especially the infra-red surface spectral properties which are not determined from the microwave retrieval.

6. Perform a surface parameter retrieval using AIRS surface sounding channels shown in Figure 1, and AMSU A and HSB window channels. This produces a new skin temperature, IR and microwave spectral emissivity, and IR spectral bi-directional inflectance. It also includes adjustment of the entire water vapor profile by a single trapezoidal function which is constant in the troposphere and lower stratosphere.

7. Determine ζ^3 taking advantages of the refined surface parameters, and produce $\hat{R}_i^3$ and new estimates of cloud parameters.

8.-11. Use $\hat{R}_i^3$ to sequentially determine surface parameters, temperature profile, humidity profile, and ozone profile. These are called the first pass retrieved products.

12. Update the temperature profile, using only AMSU A radiances and AIRS channel radiances insensitive to clouds. This profile is also used in the rejection criteria and is referred to as the test microwave only retrieval.

13. Using the first pass retrieved products and updated temperature profile, determine ζ^4,

final cloud parameters, and the final clear column radiances $\hat{R}_i^4$, which is a product of the system.

14. Repeat steps 8 and 9 using $\hat{R}_i^4$ to obtain the final product surface parameters and temperature profile. The initial guess used in the second pass surface parameter and temperature profile retrievals is identical to that of the first pass but all other parameters are updated, such as the clear column radiances, moisture profile, etc. The noise covariance matrix is also updated to account for better estimates of the other parameters. In addition, channels in the water vapor band which are highly sensitive to lower tropospheric water vapor are included in the final temperature profile step (but not the first pass) because an accurate moisture profile has now been retrieved. The moisture profile and ozone profile retrieval steps are not repeated, as no appreciable improvement in parameters resulted from further retrieval steps.

15. Test solution for acceptance. If rejected, return to the AMSU/HSB retrieval starting from the initial guess, including AIRS channels insensitive to clouds, as the "final microwave only" product. Cloud parameters for rejected cases are based on this solution and were determined in step 2.

16. Determine OLR and clear sky OLR using the appropriate solution for either accepted or rejected cases.

Adjustment of the First Guess

The first guess temperature profile $T^0(P)$ used in step 4 is usually the result of the AIRS regression done in step 3, $T^{reg}(P)$. Under most conditions, this is considerably more accurate than the microwave product $T^M(P)$ used in step 1. However, under some difficult cloud conditions, a very poor regression can be obtained. In general, the regression temperature profile will degrade below 300 mb with increasing values of the effective noise amplification factor, and can be considerably poorer than the microwave retrieval, especially near the surface. The problem is compounded, in cases of large effective noise amplification factor, because temperature sounding channels sensing the lower troposphere will be treated as noisy due to a large contribution of the second term in the noise covariance matrix (see Equation 20). Consequently, eigen functions having high vertical resolution in the lower troposphere will be heavily damped and the poor vertical structure in the lower troposphere of the regression guess will be heavily believed. To help alleviate this problem, we construct a first guess temperature profile which is a linear combination of the $T^{reg}(P)$ and $T^M(P)$ below 300 mb.

$$T^0(P) = T^{reg}(P) + A(P)\left(T^M(P) - T^{reg}(P)\right) \qquad (55)$$

where $A(P_s) = 0$ if $A_{eff} \le 2.5$ and $A(P_s) = 1$ if $A_{eff} \ge 6.5$, with values of $A(P_s)$ linearly interpolated between 0 and 1 for intermediate values of A_{eff}. In addition, $A(P) = 1$ for $P \le 300\,mb$, and $A(P)$ is linearly interpolated in ℓnP for intermediate pressure values between 300 mb and the surface pressure P_s.

Computation of OLR

Outgoing Longwave Radiation (OLR) is computed from the AIRS products in a manner analogous to that used to compute OLR from TOVS (Mehta and Susskind, 1999a, 1999b).

$$F = (1-\alpha_1-\alpha_2)F_{CLR} + \alpha_1 F_{CLD}(P_{c_1}) + \alpha_2 F_{CLD}(P_{c_2}) \qquad (56)$$

where F_{CLR}, the clear sky OLR, is the sum of contributions from 14 spectral bands each with effective surface emissivity ε_i

$$F_{CLR} = \pi \sum_{i=1}^{14}\left[\varepsilon_i B_{\nu_i}(T_s)\tau_i(P_s) + \int_{\ell nP_s}^{\ell n\bar{P}} B_{\nu_i}(\tau)\frac{d\tau_i}{d\ell nP}d\ell nP\right] = \pi\sum_i F_{i,CLR} \qquad (57)$$

and the band transmittances $\tau_i(P)$ are computed at effective zenith angles θ_i. The small term related to downwelling thermal radiation reflected off the surface and transmitted to space is neglected. $F_{CLD}(P_c)$ is computed in an analogous way, in terms of the cloud spectral emissivity $\varepsilon_i(P_c)$, and assuming a cloud transmissivity of $(1-\varepsilon_i(P_c))$

$$F_{CLD}(P_c) = \pi \sum_{i=1}^{14}\left[\begin{array}{l}\varepsilon_i(P_c)B_{\nu_i}(T(P_c))\tau_i(P_c) \\ + \int_{\ell nP_c}^{\ell n\bar{P}} B_{\nu_i}(\tau)\frac{d\tau_i}{d\ell nP}d\ell nP \\ +(1-\varepsilon_i)F_{i,CLR}\end{array}\right] \qquad (58)$$

The band transmittances $\tau_i(P)$ are parameterized as a function of temperature, moisture, and ozone profile (Mehta and Susskind, 1999b). The spectral cloud emissivity was assumed to have a constant value of 0.9, to be consistent with what was done in the cloud parameter retrieval.

Rejection Criteria

A number of tests are done to assess the quality of the retrieval. The major cause of rejection is difficulty in dealing with the effects of clouds on the AIRS radiances.

1. Assessment of Cloud Clearing Fit.

Equations 11 and 10 give the solution for the vector ζ and the resultant clear column radiances $\hat{R}_i$. If a successful solution is produced, the ensemble $\hat{R}_i$ for the cloud clearing channels i should match the incoming estimates of clear column radiances $\hat{R}_{i,CLR}$ to a reasonable degree. A poor match is indicative of either a particularly poor first guess or problems in handling the effects of clouds on the radiances. We compute the weighted residual of the clear column radiances used in the computation of ζ in brightness temperature units

$$\Delta F = \left(\frac{\sum_i (\hat{R}_i - R_{i,CLR})^2 N_{ii}^{-1}}{\sum_i N_{ii}^{-1} \left(\frac{\partial B_i}{\partial T} \right)^2_{\hat{R}_i}} \right)^{1/2} \qquad (59)$$

and reject the solution if ΔF computed when generating ζ^1 is greater than 1.75K. Equation 59 is equivalent to taking the residual of clear column brightness temperatures weighted by the channel noise covariance in brightness temperature units.

2. Difficult Cloud Cases.

Cases with extensive cloud cover and low contrast are particularly difficult. The solution is rejected if the sum of the final retrieved cloud fractions for all cloud layers is greater than 80% or the total cloud fraction is greater than 50%, and the total cloud below 500 mb is greater than 10% and the noise amplification factor is greater than 2, or the noise amplification factor is greater than 3, or the effective noise amplification factor is greater than 8. We also reject cases if the total cloud liquid water determined by the microwave product is greater than 0.03 gm/cm^2.

3. Large Residuals in Second Pass Retrievals.

The general iterative solution is terminated when either the residual R^n (Equation 44) is less than 10% of the RSS of the predicted noise for each mode $\Delta\overline{B}_\ell$, (Equation 38) or R^n is more than 75% of R^{n-1}. Slow convergence may indicate a poor solution. We reject the solution if the converged value of R is greater than the RSS of $\delta\overline{B}_\ell$ in either the surface parameter retrieval or the temperature profile retrieval in the second pass. Poor convergence generally indicates problems with the clear column radiances $\hat{R}_i^4$.

4. Inconsistency of Test "Microwave Only" and Combined IR/Microwave Retrievals.

Under some conditions, the clear column radiances $\hat{R}_i^4$ can be poor but all convergence tests are passed. Nevertheless, the test microwave only retrieval will produce low level temperatures which differ significantly from those of the second pass retrieval. This generally indicates poor clear column radiances. The solution is rejected if the RMS differences between the temperature in the lowest 3 km of the test microwave only retrieval differs from that of the second pass retrieval by more than 1.25K.

4. SIMULATION STUDY

The simulation study is based on radiances computed from conditions derived from a global simulation using a version of the operational general circulation model (GCM) from NOAA NCEP for December 15, 2000 (Juang, 1997). Details of the methodology to simulate the surface and atmospheric conditions for each AIRS footprint are given in Fishbein et al., 2002.

The test set is the first scan line of every granule (6 minute period) for December 15, 2000. The dependent data set, on which the regression coefficients are based, is taken as cloud free radiances computed from the whole day December 10, 2000. A first guess of all the geophysical parameters (including surface pressure) taken from an 18 hour GCM forecast is available for use in the retrieval. We used only the forecast surface pressure as it is felt that use of a model forecast first guess temperature-moisture profile is unnecessary to

analyze AIRS/AMSU data because of the high information content of the radiances.

The AIRS orbital dataset has the following salient features within a given scene made up of nine FOV's:

- variable surface topography and surface pressure, P_s
- daytime and nighttime conditions
- temperature, T(P), moisture, q(P), ozone, O_3(P), and other trace constituents from the surface to 0.005 mb
- cloud liquid water profiles, $\ell(P)$, (only affects microwave)
- multiple level cloud conditions within a FOV, with spectrally varying cloud emissivity, $\varepsilon_{cld}(\upsilon)$, and reflectivity, $\rho_{cld}(\upsilon)$, consistent with atmospheric conditions. The cloud top pressure, emissivity, and reflectivity are spatially varying as well.
- variable surface skin temperature, T_s, spectral surface emissivity, $\varepsilon(\upsilon)$ and spectral surface bi-directional reflectance, $\rho(\upsilon)$.
- variable land fraction, with coastlines, islands, lakes, etc.
- orbital simulation with simulated scan lines with variable viewing angle and solar zenith angle.

5. RESULTS

There were a total of 7200 cases in the simulation. In 74 cases, the microwave retrieval step failed, and no retrieval was attempted. Of the remainder, 4604 cases were accepted. Figure 2 shows the number of cases, and percent accepted, as a function of fractional cloud cover, in 0.5% bins. We also show statistics for cases we classify as "essentially clear" based on the observed radiances. This "essentially clear" flag can be of use to the data assimilation community, in which it is common to assimilate observed channel radiances under clear conditions. The data assimilation community avoids cloud contaminated radiances out of fear that noise due to handling effects of clouds on the radiances may degrade the resultant analyzed fields. Two potential problems with this approach are that only a small number of cases are completely clear, thus limiting the utility of the sounding data in improvement of forecast skill, and scenes with small amounts of cloud cover may be mistakenly classified as clear. Our "essentially clear" flag is designed to include cases of very small amounts of cloudiness to increase the yield of cases to be assimilated as compared to only 100% clear situations.

A case is a candidate to be called essentially clear if the largest eigenvalue of $\Delta R^T N^{-1} \Delta R$ is less than 125 for ocean cases and 225 for land cases. This indicates a small amount of variability in the radiances in the 3x3 array of AIRS spots. A larger value of radiance variability is allowed for land cases to be called clear because surface variability is larger over land than ocean. We also define a cloud correction value, ΔBT, as the average difference of the reconstructed clear column brightness temperature, $\hat{\Theta}_i$, and the 9 spot average brightness temperature, $\overline{\Theta}_i$, for all channels in the window regions between 800 cm^{-1} and 900 cm^{-1}. For the scene to be declared "essentially clear", ΔBT must be less than or equal to 0.1K. In addition, the retrieval must be accepted. 431 cases were called essentially clear. Figure 2 includes the number of cases called "essentially clear" as a function of actual cloud cover. The average cloudiness of all cases was 37.14%, t he average cloudiness of all accepted cases was 31.31%, and the average cloudiness of all cases called essentially clear was 0.94%. The percentage of cases accepted drops slowly with increasing cloud cover

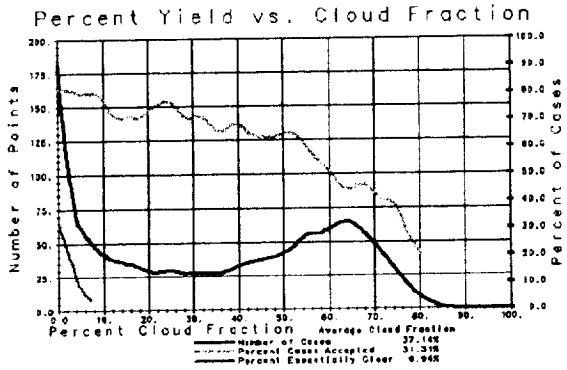

Figure 2. Number of cases as a function of cloud fraction (black), percentage of successful cases (mauve), and percentage of cases called essentially clear (blue).

until about 50%, and then drops off more rapidly after that. Roughly 40% of those accepted cases with cloud cover less than 0.5% were identified as "essentially clear."

Figure 3 shows statistics for the clear column brightness temperatures for the 431 essentially clear cases, with biases shown in Figure 3a and RMS values shown in Figure 3b. The top panel shows the difference between the noise free brightness temperatures computed from

the truth for a given scene and the average of the observed brightness temperatures in the 3x3 array of AIRS spots in the scene. This is the correction needed to make the observed brightness temperatures match the true values. The second panel shows the difference between the reconstructed brightness temperatures and the average observed values. This is the correction made in the cloud clearing. The third panel shows the difference between the reconstructed clear column brightness temperature and that computed from the truth. This is the error in the reconstructed clear column brightness temperature. Also shown in the third panel of
the RMS statistics is the single spot channel noise.

In the mean sense, "essentially clear" spots needed an average cloud correction of roughly 0.1K in the 800 cm^{-1} – 1150 cm^{-1} region, and essentially none was made on the average. This resulted in a small cold bias in this window region in the reconstructed clear column brightness temperatures. In the RMS sense, corrections of up to 0.25K were needed in the long wave window for these cases (some of this is due to channel noise) and corrections of about 0.1K were made. For the

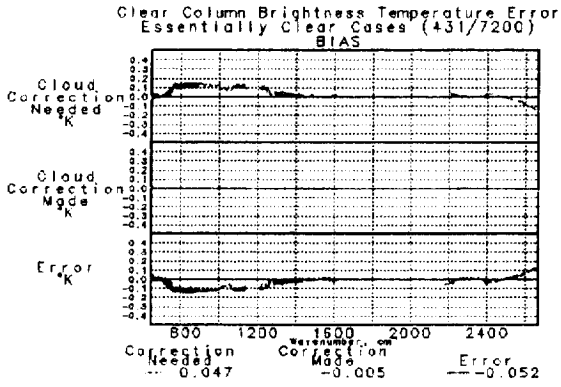

Figure 3a. Mean value of cloud correction needed, cloud correction made, and errors of cloud cleared brightness temperature for essentially clear cases.

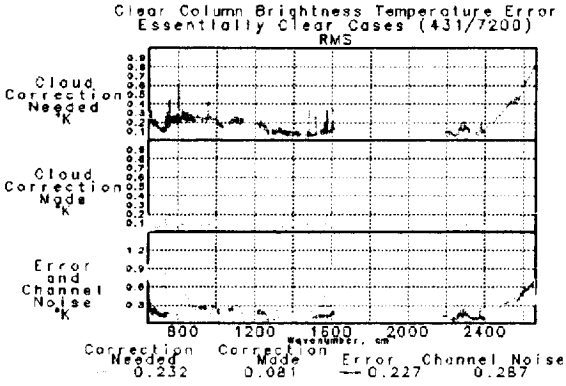

Figure 3b. RMS values of cloud correction needed, cloud correction made, and cloud cleared brightness temperature errors for essentially clear spots. Single spot noise is also shown.

most part, the RMS values of the reconstructed brightness temperatures were comparable to, or smaller than, the single spot channel noise. Lower values can arise if either the channel is considered not to see clouds (the noise amplification factor is 1/3) or the scene is considered clear or contains very small values of η, resulting in noise amplification factors less than 1, provided accurate values of η are obtained. Radiances for "essentially clear" cases are definitely suitable for data assimilation purposes.

Figure 4 shows analogous statistics for the 4604 accepted cases for all cloud conditions. On the average, cloud corrections of almost 12K were needed in the longwave window region, and the correction made was slightly smaller than needed, with about a 0.5K negative bias in reconstructed clear column brightness temperatures at the worst frequencies.

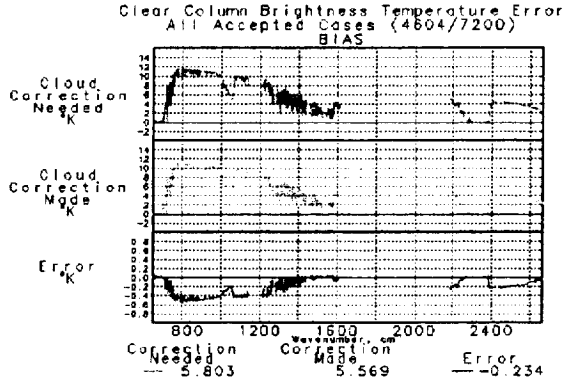

Figure 4a. Mean values of cloud correction needed, cloud correction made, and errors of cloud cleared brightness temperatures for all accepted cases.

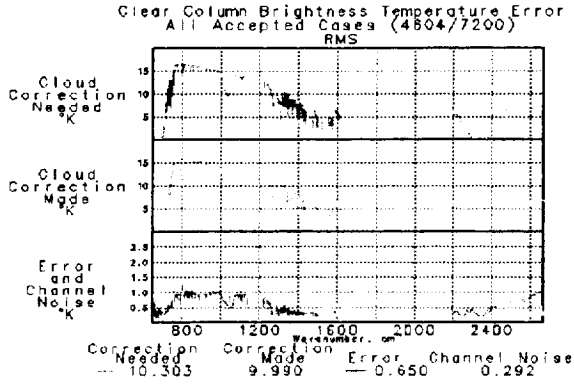

Figure 4b. RMS values of cloud correction needed, cloud correction made, and cloud cleared brightness temperature errors for all cases. Single spot noise is also shown.

In the RMS sense, reconstructed clear column brightness temperatures were still comparable to channel noise throughout most of the temperature profile sounding regions (650 cm^{-1} – 750 cm^{-1} and 2200 cm^{-1} – 2400 cm^{-1}), but larger than the noise elsewhere in the spectrum. RMS errors in the water vapor sounding region are still very small and radiances in these channels, as well as those in the temperature sounding region, should be suitable for data assimilation. We encourage researchers in the field of data assimilation to test the use of radiances for all accepted cases. This would substantially increase the number of cases which can be used and should further improve forecast skill compared to use of radiances in just clear or essentially clear cases.

Figure 5 shows RMS temperature errors for the 4604 accepted cases, as well as for the 431 essentially clear cases. Errors are shown for layer mean temperatures in roughly 1 km layers from the surface to 300 mb, 3 km layers from 300 mb to 30 mb, and 5 km layers from 30 mb to 1 mb. Results are shown for both the regression guess and the final physical retrieval. Errors of the surface skin temperature are indicated in the figure, as well as average RMS temperature profile errors over the layers 700 mb to the surface and 100 mb to the surface. The physical retrieval improves considerably over the regression based retrieval in both clear and cloudy cases with the largest improvement near the surface. In cloudy cases, part of this improvement is due to use of more

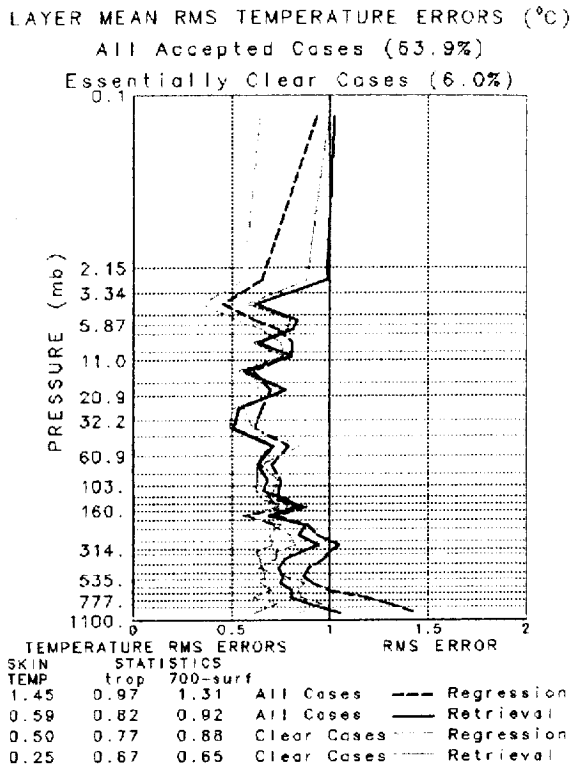

Figure 5. RMS temperature profile errors.

accurate clear column radiances as the final physical retrieval uses η^4 while the regression uses η^1. This is not a factor in clear cases however, which still show significant improvement in RMS errors near the surface. Retrievals under the multi layer cloud cover used in this simulation (average cloudiness of the accepted cases is 31%) degrade over those in clear situations beneath 150 mb, but are still of high accuracy. Average tropospheric RMS errors are 0.82K, and average lower tropospheric errors are 0.92K, both exceeding or essentially meeting the 1K RMS error requirement for AIRS. The RMS error in the lowest 1 km (1.06K) slightly exceeds 1K however. Skin temperature errors are 0.25K for clear cases and 0.59K for all cases. These include land cases and are affected by uncertainties in surface spectral emissivity.

Figure 6 shows mean and RMS errors of retrieved surface skin temperature and 1 km tropospheric layers up to 344 mb for accepted retrievals as a function of actual cloud cover. Also shown is the mean and RMS clear column brightness temperature error for the 937.8 cm^{-1} window channel. Mean and RMS errors for most temperatures are not very sensitive to cloud fraction. Negative biases are

found, which increase slowly with increasing cloud cover, for the long wave window channel radiance, the surface skin temperature, and the temperature in the lowest km of the atmosphere. RMS errors of all parameters increase slowly with increasing cloud cover, especially for the lowest km of the atmosphere.

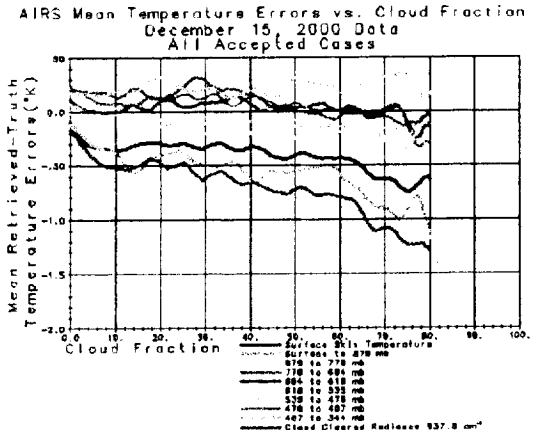

Figure 6a. Mean temperature errors as a function of cloud cover for accepted retrievals.

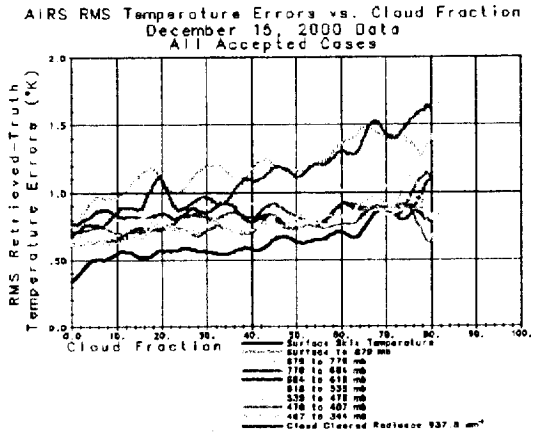

Figure 6b. RMS temperature errors as a function of cloud cover for accepted retrievals.

Figure 7 shows RMS percent errors of the retrievals, weighted by water vapor amount in the layer, for integrated column water vapor in roughly 1 km layers from the surface to 200 mb. The RMS percent errors of total precipitable water are also indicated in the figure. Clouds do not degrade the retrieval profile accuracy appreciably. Part of this result may be due to sampling differences between clear and cloudy areas.

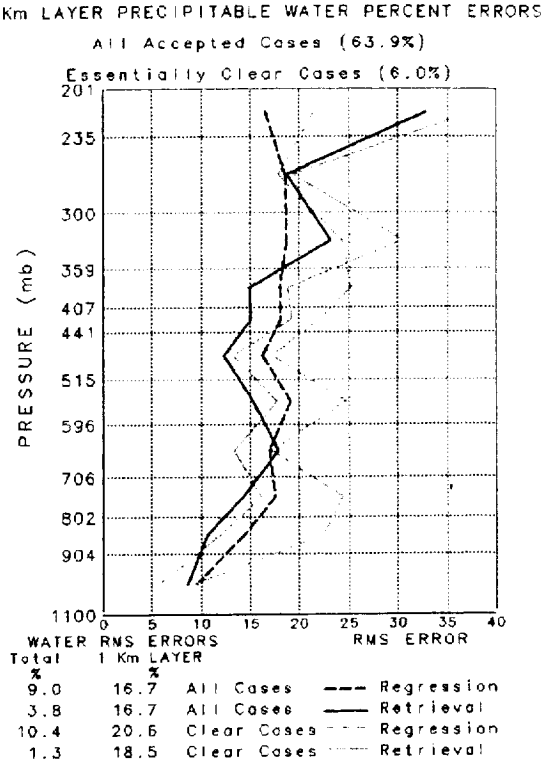

Figure 7. RMS humidity profile % errors.

Clouds degrade the total precipitable water accuracy by 2.5%, but the 3.8% error of total precipitable water for all cases is still extremely good. 1 km layer precipitable water errors in the troposphere are generally better than 20% in the cloudy cases in layers up to about 235 mb. Clear cases RMS % errors appear worse than all case errors in the upper troposphere. This is probably the result of clear cases being considerably dryer than cloudy cases and more difficult to retrieve on a percentage basis.

Figure 8 shows weighted percent errors in the ozone profile retrievals in roughly 4 km layers from 260 mb to 2.15 mb and in one coarse layer from 260 mb to the surface. Also shown is the percentage error in total ozone, which is 2.4% for clear cases and 2.6% for cloudy cases. The RMS profile errors are better than 8% in all layers in both clear and cloudy cases. The physical retrieval improves tropospheric ozone retrievals considerably over what is obtained by regression.

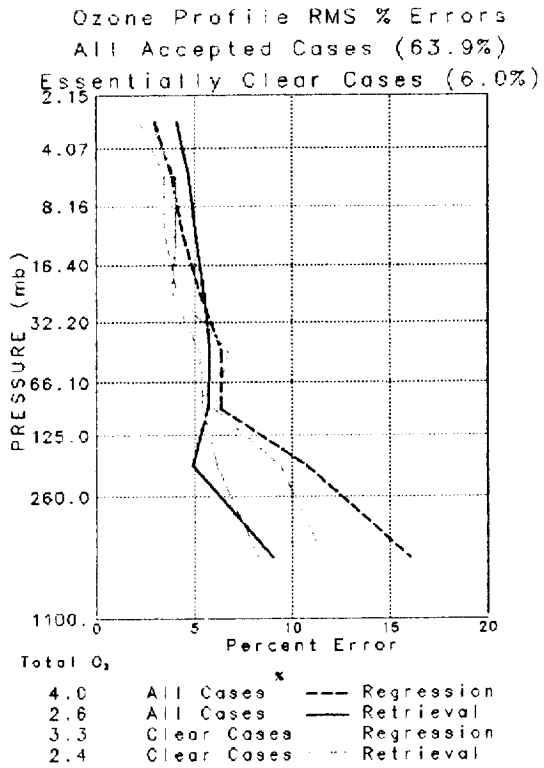

Figure 8. Ozone profile retrieval errors.

The accuracy of cloud parameters cannot be compared in a straightforward manner because of the existence of two cloud layers in some (most) scenes. The retrieved cloud fractions are effective, both because of errors in retrieved cloud top pressure and assumed cloud spectral emissivity. In the retrieval process, cloud spectral emissivity was always assumed to be 0.9 while the true cloud spectral emissivity varied a few percent from that. Two straightforward parameters to compare are total cloud fraction $\alpha_1 + \alpha_2$, and OLR. The OLR validates

the cloud parameters, as well as all other parameters, in a radiative sense. Clear sky OLR (F_{CLR}) is also useful to validate all parameters with the exception of clouds. Accuracies should be better for accepted cases than for rejected cases, because cloud products and all other parameters for rejected cases are based on the AMSU retrievals which are less accurate.

Table 4 shows statistics for retrieved cloud cover, OLR and clear sky OLR for accepted and rejected cases. The errors for rejected retrievals are poorer than for accepted retrievals, but all products should be useful for climate studies. The OLR product is complementary to OLR measured more directly from CERES, also on the Aqua platform, in that the AIRS derived product will explain variations of OLR and clear sky OLR in space and time in terms of variations of surface and atmospheric parameters, including cloud cover and height.

Table 4. Retrieved Cloud Fraction and OLR Errors

	Accepted Cases	Rejected Cases
Number	4604	2522
Average Cloud Cover	31.31%	47.12%
Bias	1.98%	-1.17%
RMS Error	6.33%	11.75%
Average OLR	221.8 W/m^2	196.2 W/m^2
Bias	-1.28 W/m^2	0.38 W/m^2
RMS Error	2.94 W/m^2	5.20 W/m^2
Average CLR OLR	253.0 W/m^2	238.8 W/m^2
Bias	-1.60 W/m^2	-1.81 W/m^2
RMS Error	2.57 W/m^2	6.76 W/m^2

REFERENCES

Aumann, H., M. Chahine, C. Gautier, M.Goldberg, E. Kalnay, L. McMillin, H. Revercomb, P. Rosenkranz, W. Smith, D. Staelin, L. Strow, and J. Susskind, "AIRS/AMSU/HSB in the Aqua Mission, Design, Science Objectives, and Data Products." IEEE Rem. Sens., 2002.

Backus, G. and E. Gilbert, "Uniqueness in the Inversion of Inaccurate Gross Earth Data." Phil. Trans. Royal Soc. London, A266, 123-192, 1970.

Chahine, M. T. and J. Susskind, Fundamentals of the GLA Physical Retrieval Method. Report on the Joint ECMWF/EUMETSAT workshop on the use of satellite in Operational Weather Prediction: 1989-1993. A. Hollingsworth Editor, Vol. 1, 171-300, 1989.

Chahine, M. T., "Remote Sounding of Cloudy Atmospheres. I. The Single Cloud Layer." J. Atmos. Sci., 31, 233-243, 1974.

Chahine, M. T., "Remote Sounding of Cloudy Atmospheres. II Multiple Cloud Formations." J. Atmos. Sci., 34, 744-757, 1977.

Chahine, M. T., "Determination of the Temperature Profile in an Atmosphere from its Outgoing Radiance." J. Optic. Soc. Amer., 58, 1634-1637, 1968.

Cuomo, V., R. Rizzi, and C. Serio, "An Objective and Optimal Estimation Approach to Cloud-Clearing for Infrared Sounder Measurements." Int. J. of Rem. Sensing, 14, 729-743, 1993.

Eyre, J. R., "Inversion of Cloudy Satellite Sounding Radiances by Non-Linear Optimal Estimation. I: Theory and Simulation for TOVS." Q.J.R. Meteorol. Soc., 115, 1007-1026, 1989a.

Eyre, J. R., "Inversion of Cloudy Satellite Sounding Radiances by Non-Linear Optimal Estimation. II: Application to TOVS Data." Q.J.R. Meteorol. Soc., 115, 1027-1037, 1989b.

Eyre, J. R., "The Information Content of Data from Satellite Sounding Systems: A Simulation Study." Q.J.R. Meteorol. Soc., 116, 401-434, 1990.

Fishbein, E. D. Gregorieh, M. Gunson, M. Hofstadter, S. Y. Lee, P. W. Rosenkranz, and L. Strow, "The Atmospheric Infrared Sounder (AIRS) Simulation System." IEEE Rem. Sensing, 2002.

Goldberg, M. D., L. M. McMillin, W. Wolff, L. Zhou, Y. Qu, and M. Divakerla, "AIRS Near Real-Time Products in Support of Global Data Assimilation for Medium Range Weather Forecasting." IEEE Rem. Sens., 2002.

Hanel, R. A., B. J. Conrath, D. E. Jennings, and R. E. Samuelson, "Exploration of the Solar System by Infrared Remote Sensing." Cambridge University Press, Cambridge, Great Britain, 1992.

Juang, H-M., S. Y. Hong, and M. Kinamitsu, "The NCEP Regional Spectral Model: An Upate." Bull. Am. Meteor. Soc., 78, 2125-2128, 1997.

Kaplan, L. D., M. T. Chahine, J. Susskind, and J. E. Searl, "Spectral Band Passes for a High Precision Satellite Sounder." Appl. Opt., 16, 322-325, 1977.

Mehta, A. and J. Susskind, "Outgoing Longwave Radiation from the TOVS Pathfinder Path A Data Set." J. Geophys. Res., 104, 12193-12212, 1999a.

Mehta, A. and J. Susskind, "Longwave Radiative Flux Calculations in the TOVS Pathfinder Path A Data Set." NASA CR 1999-208643, Greenbelt, Md., 1999b.

McMillin, L. M., and C. Dean, "Evaluation of a New Operational Technique for Producing Clear Radiances." J. Appl. Meteor., 21, 1005-1014, 1982.

Rodgers, C. D., Retrieval of Atmospheric Temperature and Composition from Remote Measurements of Thermal Radiation. Rev. Geophys. and Space Phys., 14, 609-624, 1976.

Rosenkranz, P. W., "Retrieval of Temperature and Moisture Profiles from AMSU-A and AMSU-B Measurements." IGARSS, 2000.

Rosenkranz, P. W., "Radiative Transfer and Rapid Forward Model for AMSU/HSB Channels." IEEE Rem. Sens., 2002.

Smith, W. L., "An Improved Method for Calculating Tropospheric Temperature and Moisture from Satellite Radiometer Measurements." Mon. Wea. Rev., 96, 387-396, 1968.

Strow, L., S. Hannon, S. Desouza-Machado, D. Tobin, and H. Motteler, "AIRS Radiative Transfer Algorithm Development and Validation." IEEE Rem. Sens., 2002.

Susskind, J., C. Barnet, and J. Blaisdell, "Determination of Atmospheric and Surface Parameters from Simulated AIRS/AMSU/HSB Sounding Data: Retrieval and Cloud Clearing Methodology." Adv. Space Res., 21, 369-384, 1998.

Susskind, J., P. Piraino, L. Rokke, L. Iredell, and A. Mehta, Characteristics of the TOVS Pathfinder Path A Data Set. Bull. Am. Met. Soc., 78, 1449-1472, 1997.

Twomey, S., "On the Numerical Solution of the Fredholm Integral Equations of the First Kind by Inversion of the Linear System Produced by Quadrature." J. Assoc. Comp. Mach., 10, 79-101, 1963.